BAU Journal - Science and Technology

Volume 1 | Issue 1
ISSN: 2706-784X

Article 6

December 2019

# INFLUENCE OF NANO-AG ADDITION ON PHASE FORMATION AND EXCESS CONDUCTIVITY ANALYSIS OF (CU0.5TL0.5)-1223 SUPERCONDUCTING PHASE

Nayera Mohammed
*Faculty of Science, Alexandria University, Alexandria, Egypt*, nysharaf@yahoo.com

Seham Mahmoud
*Faculty of Science, Alexandria University, Alexandria, Egypt*, gomaagaber@hotmail.com

Weleed Abdeen
*Faculty of Science, Alexandria University, Alexandria, Egypt & University College at Al-Gamom, Umm Al-Qura University, Saudi Arabia*, waabdeen@uqu.edu.sa

Marwa Hasebbo
*Faculty of Science, Alexandria University, Alexandria, Egypt*, marwahaseboo@yahoo.com

# INFLUENCE OF NANO-AG ADDITION ON PHASE FORMATION AND EXCESS CONDUCTIVITY ANALYSIS OF (CU0.5TL0.5)-1223 SUPERCONDUCTING PHASE


## Abstract

Ceramic superconducting samples of type (nano-Ag)xCu0.5Tl0.5Ba2Ca2Cu3O10-δ, 0.0 ≤ x ≤ 3.0 wt.%, were successfully synthesized via single step solid-state reaction technique at 850 ºC and under ambient pressure. The samples were characterized by XRD and SEM. Obtained data revealed that the highest grains connectivity volume fraction was detected for the sample with x = 0.15 wt.%. The electrical properties of the prepared samples was examined using the electrical resistivity measurements, and the results proved that the highest superconducting transition temperature Tc was observed at x = 0.15 wt.%. Furthermore, the fluctuation conductivity Δσ(T), above Tc, was analyzed as a function of reduced temperature, t=(T-T_c^mf)/(T_c^mf ), using Aslamazov and Larkin (AL) theory and its modified form given by Lawrence-Doniach (LD) model. Excess conductivity analysis showed crossover between two dimensional (2D) to three-dimensional (3D) with decreasing temperature for all samples. The highest crossover temperature T2D-3D was observed for x = 1.5 wt.%, which showed the smallest coherence length along c-axis ξ(0), Fermi velocity vF, Fermi energy EF and interlayer coupling ν in these samples.



## Keywords

Nano-Ag, (Cu0.5Tl0.5)–1223, Excess conductivity.

## 1. INTRODUCTION

Cu-1223 phase prepared at 4GPa with $T_c$ = 68 K and Γ about 1.7 [1-3]. Regrettably, such preparation impedes Cu-1223 from a wide range of applications. Replacing Tl at the Cu atoms in the charge reservoir layer develops $(Cu_{1-x}Tl_x)$-1223 that can be synthesized at normal pressure. This compound is characterized by low Γ, high critical current density $J_c$ and high superconducting transition temperature $T_c$ [4, 5]. One of a promising application is $(Cu_{0.5}Tl_{0.5})$-1223, because of its amazing electrical properties, such as high values of $T_c$ (113-132 K) and $J_c$, and values of low values of Γ (Γ = 4) [4]. The crystal structure of $(Cu_{0.5}Tl_{0.5})$-1223 with P4/mmm space group with tetragonal unit cell [6]. This phase consists of 3 $CuO_2$-planes and a semi insulating charge reservoir layer $(Cu_{0.5}Tl_{0.5})Ba_2O_{4-\delta}$ in its unit cell.

The study of the excess conductivity attributable to thermal fluctuations is crucial for knowing the intrinsic superconducting characteristics and dimensionality of HTSCs. Superconducting properties depend on both the intrinsic properties such as conduction dimensionality and coherence lengths, and the extrinsic properties such as the grain morphology of the samples. The excess conductivity is analyzed by several models such as Aslamazove and Larkin (AL), Maki-Thompson (MT), Lawrence and Doniach (LD) and Hikami-Larkin (HL) [7-10]. AL theory and LD model were applied to study the excess conductivity of different samples by several groups [11-21]. In AL model, the excess conductivity originates from the formation of Cooper pairs above $T_c$. The LD model is the modification of AL theory for polycrystalline samples that expecting a crossover from 2D to 3D conductivity, as temperature move towards $T_c$. On other hand and according to MT model, the excess conductivity arises from the scattering of fluctuating pairs from conventional electrons and hence described the region of abstemious pair breaking.

By adding nano-particles to HTSCs, there is a great chance for enhancing the flux pinning and $J_c$ values, since the size of nano-particles is greater than the coherence length ξ and smaller than the penetration depth λ, leading to powerful interaction between flux line network and nano-particles. A proper addition of nano-particles such as $ZrO_2$ [22], $Al_2O_3$ [23, 24], and $NiFe_2O_4$ [25] in (Bi,Pb)-2223, and $ZrO_2$and ZnO [26] in Gd-123 acted as effective flux pinning centers and improved $J_c$. Also, nano-particles addition to $(Cu_{0.5}Tl_{0.5})$-1223, such as $SnO_2$ [27], $In_2O_3$ [27] and $Fe_2O_3$ [28], lowered porosity and improved both, volume fraction and Vickers microhardness. Moreover, adding nano-particles of CuO, BaO and $CaO_2$ [29] to $(Cu_{0.5}Tl_{0.5})$-1223 improved superconducting properties such as $T_c$, intergrain connectivity and magnitude of diamagnetism. adding low amounts of nano-ZnO to $(Cu_{0.5}Tl_{0.25}Pb_{0.25})$-1223 [30] enhanced the volume fraction, $T_c$, $J_c$ and the melting temperature. The superconducting parameters of Gd-123 [31] added with nano-$CoFe_2O_4$, Y-123 [32] added with $Zn_{0.95}Mn_{0.05}O$ and ZnO, and CuTl-1223[33] added with nano-CuO were determined from excess conductivity. The results showed that the low concentration of nano-sized addition improved $J_c$ and the critical magnetic fields ($B_c$, $B_{c1}$ and $B_{c2}$) and inter-grain coupling ν.

The present work analyzed the impact of adding nano-Ag to the phase formation and the behavior of thermal fluctuations conductivity above $T_c$. The superconducting parameters such as $\xi_c(0)$, $v_F$, $E_F$ and ν of $(Cu_{0.5}Tl_{0.5})$-1223 superconducting phase were calculated. For this study, superconducting samples of type $Cu_{0.5}Tl_{0.5}Ba_2Ca_2Cu_3O_{10-\delta}$ with different concentrations of nano-Ag addition were prepared and investigated using XRD, SEM and electrical resistivity measurement.

## 2. EXPERIMENTAL TECHNIQUE

Superconducting samples of type Cu0.5Tl0.5Ba2Ca2Cu3O10-δ added with nano-Ag were synthesized using single step solid-state reaction technique. Grinding stoichiometric ratios of oxides of Tl2O3, BaO2, CaO, and CuO, of high purity, in agate mortar. To and get a homogenous mixture, the grinded powder were twice sifted using 85 μm sieve. Finally, nano-Ag (Aldrich, 20-40 nm) was mixed with different amounts (0.0, 0.5, 1.0, 1.5, 2.0 and 3.0 wt.%) with the resulted powder. Then, the obtained powder pressed into a disc of 15 mm diameter and a thickness of about 3 mm. The pressed disc was wrap up in a silver foil to decrease the loss in thallium through preparation. Then, disc was heated in sealed quartz tubes (7.5 mm radius and 120 mm length) at 4 oC/min to 760 oC, followed by heating to 850 oC at 2 oC/min, then the samples held at 850 oC for 5 hours. Slowly cooling to room temperature, by furnace cooling is the last stage.

Sample characterization and the electrical resistivity measurements where discussed in a previous work [17].

## 3. RESULTS AND DISCUSSION

The XRD patterns of (nano-Ag)xCu0.5Tl0.5Ba2Ca2Cu3O10-δ, with 0.0 ≤ x ≤ 3.0 wt.% are shown in Fig. 1. The XRD patterns of the samples with x ≤ 2.0 wt.% indicate the formation of a single of (Cu0.5Tl0.5)-1223 with tetragonal P4/mmm symmetry. Small quantities of secondar phases are appeared, such as (Cu0.5Tl0.5)-1212 and Ba2Cu3O5.9. On the other hand, XRD patterns of (nano-Ag)3.0wt.%Cu0.5Tl0.5Ba2Ca2Cu3O10-δ sample indicate the formation of (Cu0.5Tl0.5)-1212 phase with space group P4/mmm and tetragonal unit cell [34], with small amount of BaCuO2. This means that a phase change from (Cu0.5Tl0.5)-1223 phase to (Cu0.5Tl0.5)-1212 phase occurred at x = 3.0 wt.%. Similar result was noted for Y-123 when adding Ag, that might substitute Cu [35], and when added by nano-Al2O3 that could fill Y and Cu(1) sites [36], and for (Bi,Pb)-2223 phase when adding high amounts of nano-SnO2 that changes (Bi,Pb)-2223 to (Bi,Pb)-2212 phase [37]. It should me mentioned that no peaks corresponds to nano-Ag or Ag-based compounds were detected by X-ray diffraction. Similar results were noticed for (Cu0.5Tl0.5)-1223 added by nano-SnO2 [38] and nano-CuO [33] and for (Bi,Pb)-2223 added by nano-NiFe2O4 [25].

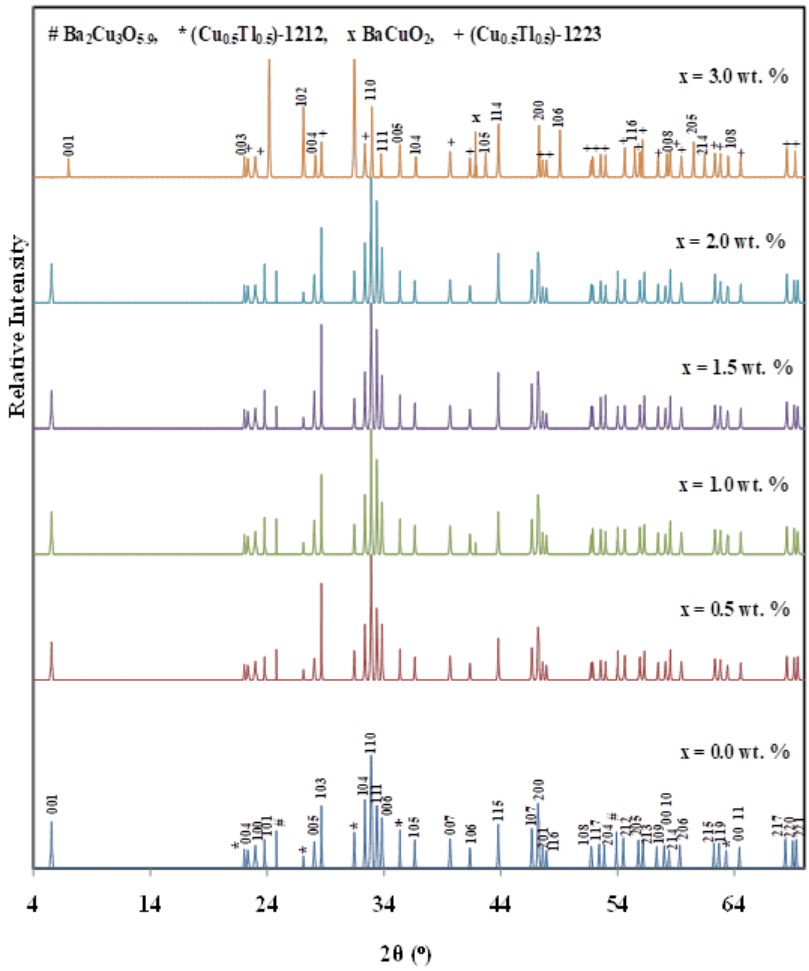


Fig.1: The XRD patterns for (nano-Ag)$_x$Cu$_{0.5}$Tl$_{0.5}$Ba$_2$Ca$_2$Cu$_3$O$_{10-\delta}$, 0.0 ≤ x ≤ 3.0 wt.%.

The calculated volume fractions are listed in table 1. It is clear that the volume fraction of (Cu0.5Tl0.5)-1223 increases as the x increases up to 1.5 wt.% and then it decreases, so the high addition retards the formation rate of (Cu0.5Tl0.5)-1223 phase. Hence, the viscosity of the forming transient liquid at the reaction temperature is affected by the addition of nano-Ag, its homogeneity and hence the phase formation rate were also affected. Similar trend were noticed for (Bi,Pb)-2223 phase, when adding nano-Al2O3 [24], and when also, adding nano-MgO [39] and for (Cu0.25Tl0.75)-1234 phase added by nano-MgO [40].

Table 1. The volume fractions percentage of $(Cu_{0.5}Tl_{0.5})$-1223, $(Cu_{0.5}Tl_{0.5})$-1212, $Ba_2Cu_3O_{5.9}$ and $BaCuO_2$ phases and the lattice parameters for $(nano\text{-}Ag)_xCu_{0.5}Tl_{0.5}Ba_2Ca_2Cu_3O_{10-\delta}$ with x

| **x** | **The volume fractions (%)** | | | | **The lattice parameters** | |
|---|---|---|---|---|---|---|
| **(wt.%)** | $(Cu_{0.5}Tl_{0.5})$-1223 | $(Cu_{0.5}Tl_{0.5})$-1212 | $Ba_2Cu_3O_{5.9}$ | $BaCuO_2$ | *a* (Å) | *c* (Å) |
| **0.0** | 88.23 | 6.36 | 5.41 | 0.00 | 3.850 (1) | 15.888 (2) |
| **0.5** | 89.61 | 5.59 | 4.75 | 0.00 | 3.852 (1) | 15.887 (3) |
| **1.0** | 90.03 | 5.50 | 4.47 | 0.00 | 3.852 (2) | 15.882 (3) |
| **1.5** | 91.55 | 5.29 | 3.16 | 0.00 | 3.851 (1) | 15.885 (3) |
| **2.0** | 89.61 | 5.59 | 4.80 | 0.00 | 3.850 (1) | 15.884 (4) |
| **3.0** | 35.20 | 61.65 | 0.00 | 3.15 | 3.850 (1) | 12.697 (7) |

The least squares method is used to determine the lattice parameters "a" and "c", that are recorded in table 1. From these results, it is clear that no considerable difference between the lattice constants for samples with $x \leq 2.0$ wt.% with respect to the sample with x = 0.0 wt.%. This can be explained as nano-Ag does not enter the (Cu0.5Tl0.5)Ba2Ca2Cu3O10-δ crystal structure. Similar results were noticed for (Bi,Pb)-2223 when adding nano-Gd [41], and nano-NiFe2O4 [25], and for (Cu, Tl)-1223 added by nano-ZnFe2O4 [42]. For x = 3.0 wt.%, "c" reduces to become nearer to that of (Cu0.5Tl0.5)-1212 [34]. This behavior suggests that Cu site could be filled by Ag. Similar conclusion was noticed for Y-123 when adding Ag [36] and nano-Al2O3 [37].

Typical SEM micrographs for (nano-Ag)xCu0.5Tl0.5Ba2Ca2Cu3O10-δ, for x = 0.0, 0.5, 1.5 and 3.0 wt.% are shown in Figs. 2(a), (b), (c) and (d), respectively. The micromorphology shows that the samples have a rectangular plate shape that signify (Cu0.5Tl0.5)-1223 phase [43]. Few number of irregular shaped and spherical grains which indicate to (Cu0.5Tl0.5)-1212 phase [44] and the impurity phases Ba2Cu3O5.9 [44] and BaCuO2 [43]. It is obvious that the grains corresponds to (Cu0.5Tl0.5)-1212 phase reduce, while those (Cu0.5Tl0.5)-1223 phase raise and are more aligned up to x = 1.5 wt.%. This means that adding of small amount improves the (Cu0.5Tl0.5)-1223 phase formation. Not far from the results obtained for (Bi,Pb)-2223 phase substituted by Ag [45]. The number of irregular-shaped plates for (nano-Ag)3.0wt.%Cu0.5Tl0.5Ba2Ca2Cu3O10-δ, Fig. 2(d), increase, improving (Cu0.5Tl0.5)-1212 phase formation.

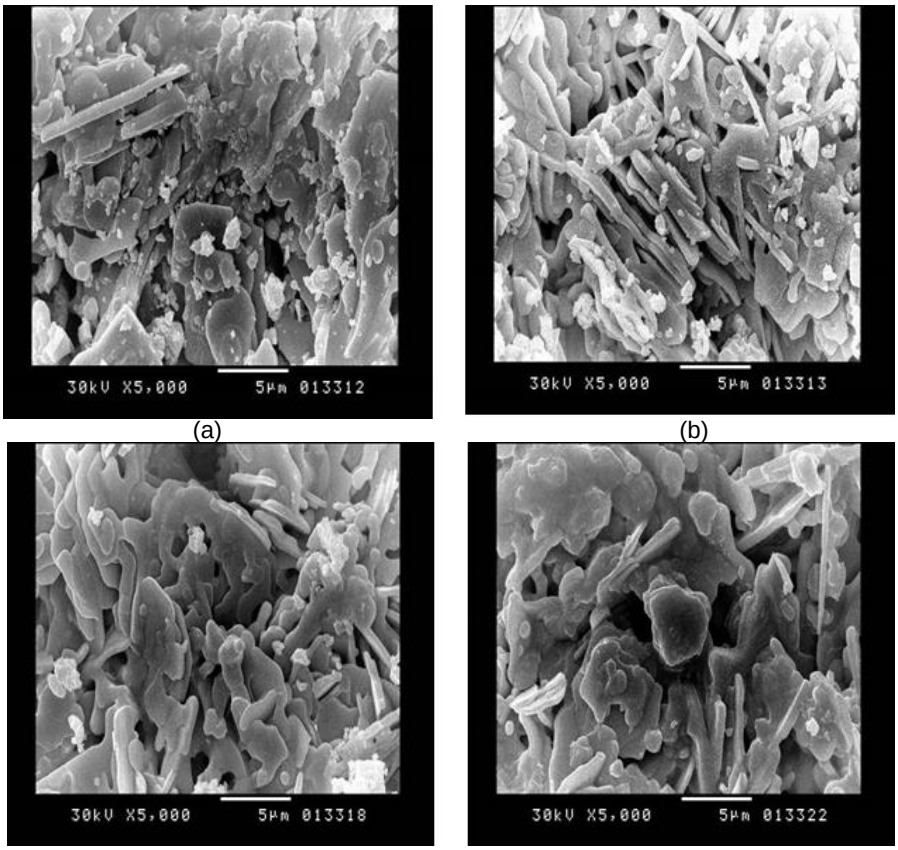


Fig. 2: SEM images for $(nano\text{-}Ag)_xCu_{0.5}Tl_{0.5}Ba_2Ca_2Cu_3O_{10-\delta}$ for x (a) 0.0 wt.%; (b) 0.5 wt.%; (c) 1.5 wt.%; (d) 3.0 wt.%.

The temperature dependence of the electrical resistivity for all prepared samples in the temperature range T0 ≤ T ≤ 300 K is shown in Fig. 3. All prepared samples show a linear behavior at high temperatures, then a sharp transition occurred as the temperature is decreased. Martin et al. [46] using the Bloch-Gruneisen formula to fit the T-linear electrical resistivity in Bi-cuprates, which gave an unreasonably low Debye temperature of less than 35 K. Bosons and fermions are quarantined to the CuO-planes, and the electrical resistivity in the plane is generated by the scattering of the bosons from fermions, which will follow the linear temperature dependence [47]. By using the marginal Fermi liquid theory by Varma et al. [48] and the nested Fermi liquid by Virosztek and Ruvalds [49], one can explain the T-linear electrical resistivity.

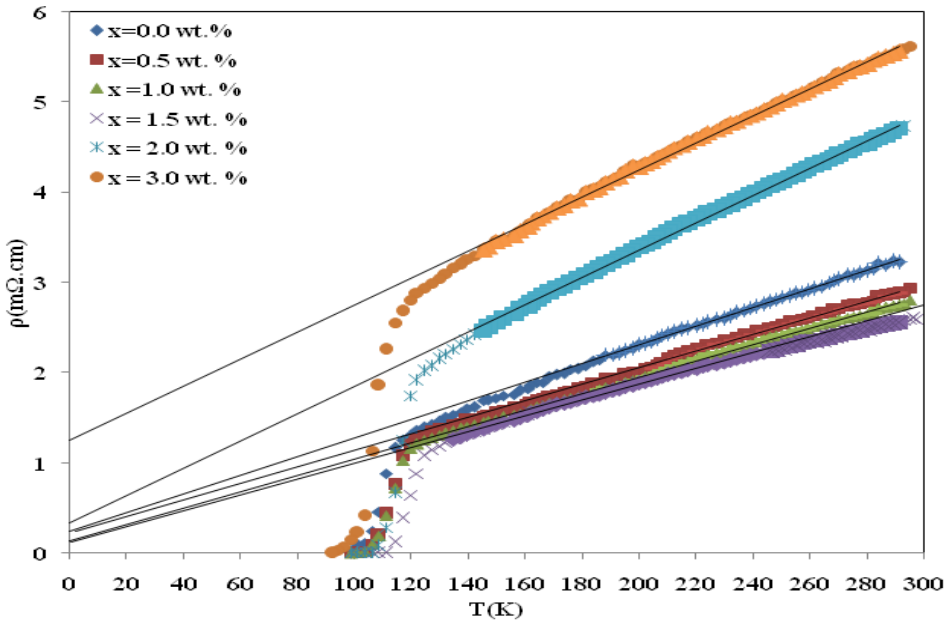


Fig.3:Temperature dependence of electrical resistivity for $(nano\text{-}Ag)_xCu_{0.5}Tl_{0.5}Ba_2Ca_2Cu_3O_{10-\delta}$, 0.0 ≤ x ≤ 3.0 wt.%.

It is clear from Fig. 3 that there is a tiny curvature in the resistivity beyond Tc that distinguishes the superconducting thermodynamic fluctuations [50]. The data for the samples with x ≤ 2.0 wt.% indicates the formation of a single phase of (Cu0.5Tl0.5)-1223, since the transition to zero resistivity temperature is sharp. While a broaden transition was noticed for the sample (nano-Ag)3.0wt.%Cu0.5Tl0.5Ba2Ca2Cu3O10-δ,, indicating the formation of secondary phase. The electrical resistivity data for all prepared samples are fitted using:

Eq (1) $\rho_n = \rho_0 + QT$, where Q is resistivity temperature coefficient and ρ0 is residual resistivity. Table 2 summarizes ρn, ρ0, Q, Tc and the transition width ΔT.

Table 2: Variation of $\rho_n$, $\rho_0$, Q, $T_c$, ΔT and $T_c^{mf}$ with nano-Ag additions

| x (wt.%) | $\rho_n$ (mΩ.cm) | $\rho_0$ (mΩ.cm) | Q (mΩ.cm.K$^{-1}$) | $T_c$ (K) | ΔT = $T_c$- $T_0$ (K) | $T_c^{mf}$ (K) |
|---|---|---|---|---|---|---|
| **0.0** | 3.225 | 0.242 | 0.010 | 111.27 | 12.77 | 112 |
| **0.5** | 2.879 | 0.231 | 0.009 | 114.34 | 10.84 | 115.40 |
| **1** | 2.747 | 0.141 | 0.009 | 114.34 | 10.84 | 115.60 |
| **1.5** | 2.559 | 0.125 | 0.008 | 120.33 | 9.33 | 121.20 |
| **2.0** | 4.706 | 0.337 | 0.014 | 117.29 | 11.29 | 117.60 |
| **3.0** | 5.558 | 1.252 | 0.015 | 107.87 | 15.28 | 108.00 |

It is clear that both ρn and ρ0 decrease with increasing x till 1.5 wt.%, then they increase as x increases. The reduction in ρn could be attributed to the diffusion of nano-Ag over the pore surfaces and the grain boundaries. Similar results noticed for Bi-2223 phase added byAg2CO3 [51] and for Y-123 phase added by nano-Al2O3 [37]. These results are in good agreement with those obtained from SEM. While the rise of ρn may be due to the rise in the grain boundaries and impurities scattering. The small values of ρ0 indicate that the high quality of the prepared samples and have less defects.

These results are in good agreement with results determined from X-ray and scanning electron microscopy. The resistivity temperature coefficient values change slightly till x = 1.5 wt.%, that could be explained as the nano-Ag additions don't alter the charge carriers-concentrations, since it does not enter the crystal structure of (Cu0.5Tl0.5)-1223. The increase in the resistivity temperature coefficient may be attributed to the phase change and the reduction in the charge carriers-concentrations. It is well known that the granular HTSC's have a well-defined Tc. It is determined from the first derivative of ρ(T) with respect to the temperature, and the maximum of dρ(T)/dT corresponds to Tc [52], which are shown in the Fig. 4 and listed in table 2. It is clear that the superconducting transition temperature values increase as x increasing up to 1.5 wt.% which may be described according to the increase in the volume fraction of (Cu0.5Tl0.5)-1223. The decrease of Tc for x > 1.5 wt.% may be due to the phase change from (Cu0.5Tl0.5)-1223 phase to (Cu0.5Tl0.5)-1212 phase or the blocking of mobile holes [37]. Table 2 shows the effect of different nano-particles SnO2 [27], In2O3 [27] and Fe2O3 [28] addition on enhancement of Tc and volume fraction for (Cu0.5Tl0.5)-1223 superconducting phase. It is obvious that there is no direct relation between the increase of Tc and volume fraction. So, the increase in the volume fraction is not the main factor for increasing Tc. This suggested that the alignment of grains and grains connectivity could play the roles for enhancing Tc. Abou-Aly et al. [53] noted similar results, who found that the maximum improvement of Tc for (Bi,Pb)-2223 when adding by nano-SnO2.

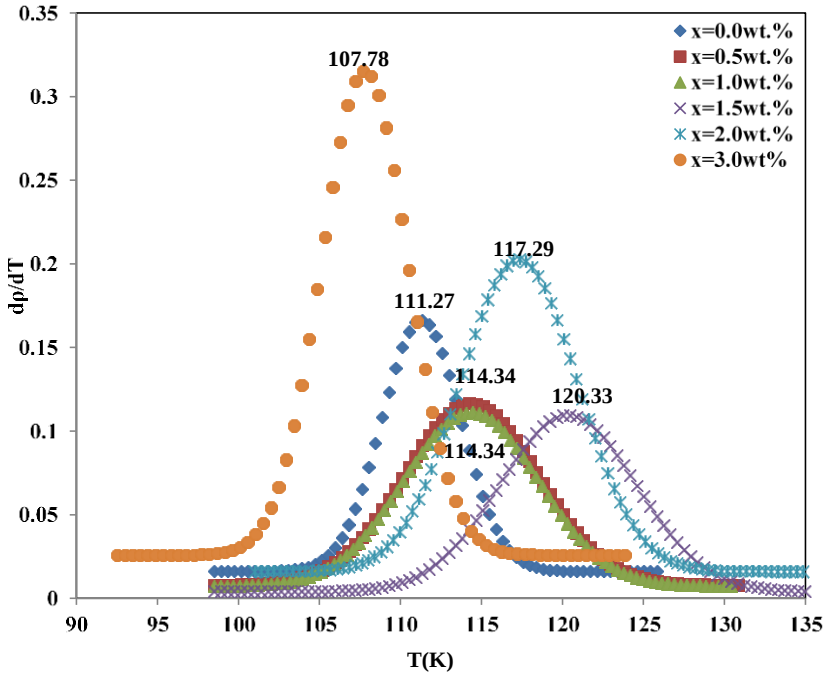


Fig.4: $\frac{d\rho}{dT}$ versus T for (nano-Ag)$_x$Cu$_{0.5}$Tl$_{0.5}$Ba$_2$Ca$_2$Cu$_3$O$_{10-\delta}$, $0.0 \leq x \leq 3.0$ wt.%.

The excess conductivity for (nano-Ag)$_x$Cu$_{0.5}$Tl$_{0.5}$Ba$_2$Ca$_2$Cu$_3$O$_{10-\delta}$, with $0.0 \leq x \leq 3.0$ wt.% above $T_c$ was studied in the scope of AL theory and LD model. The excess conductivity is expressed as:

Eq (2) $\Delta\sigma_{AL} = At^{\alpha}$

where, t is a reduced temperature $\left(t = \frac{T - T_c^{mf}}{T_c^{mf}}\right)$, $T_c^{mf}$ is mean field critical temperature, α is the dimensional exponent, α = -0.3, for cr fluctuations, α = -0.5 for 3D fluctuations and α = -1.0 for 2D fluctuations that follows the relationship; Dimensionality $D = 2\{2 + \alpha(D)\}$ [54]. A is the temperature independent parameter has two values, $\frac{e^2}{32\,\eta\,\xi_c(0)}$ for 3D where, $\xi_c(0)$ is the zero-temperature coherence length along the c-axis and $\frac{e^2}{16\,\eta\,d}$ for 2D where, d is the effective layer thickness of superconducting layers (d ~ 15 Å for (Cu$_{0.5}$Tl$_{0.5}$)-1223 and ~ 12 Å for (Cu$_{0.5}$Tl$_{0.5}$)-1212).The temperature at which a crossover from three to two dimensional takes place is given by;

Eq (3) $T_{LD} = T_c^{mf}\left\{1 + \left(\frac{2\,\xi_c(0)}{d}\right)^2\right\}$

The excess conductivity Δσ induced by thermal fluctuation is calculated by:

Eq (4) $\Delta\sigma = \sigma_m(T) - \sigma_n(T)$,

where, $\sigma_m(T)$ and $\sigma_n(T)$ are the measured and normal state extrapolated conductivity, respectively. $T_c^{mf}$ values are determined by extrapolation of straight line in $\Delta\sigma^{-2}$ versus T plots shown in Figs. 5(a), (b) and (c) and they are recorded in table 3. This method was reported by Han et al. [55] considering the 3D behavior of an anisotropic superconductor near $T_c$ when $\xi_C(T) = \xi_C(0)t^{-1/2}$ become large. In this region $\Delta\sigma \approx t^{-1/2}$ so $\Delta\sigma^{-2}$ versus T should be a straight line approaching zero when $T \rightarrow T_c^{mf}$. $T_c^{mf}$ values for our samples are of about 0.13 (x = 3 wt.%) and 1.26 (x = 1.0 wt.%) higher than the values of $T_c$.

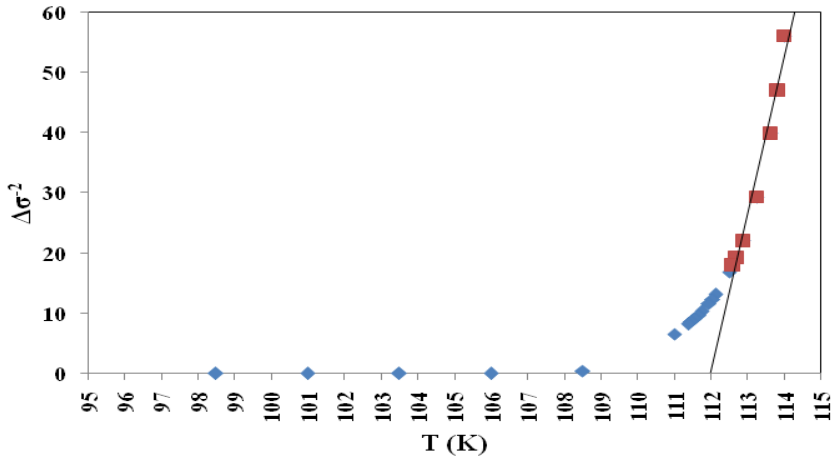


(a)

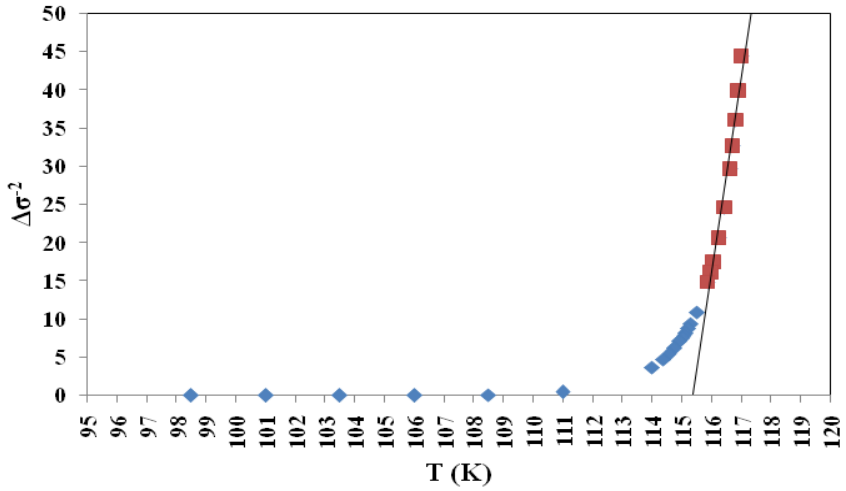


(b)

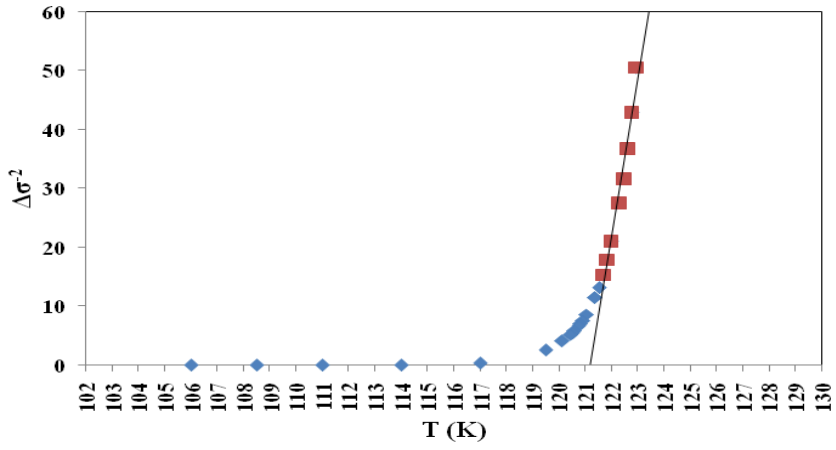


(c)

Fig. 5: The variation of $\Delta\sigma^{-2}$ versus T for (nano-$Ag)_xCu_{0.5}Tl_{0.5}Ba_2Ca_2Cu_3O_{10-\delta}$ with x: (a) 0.0 wt.%; (b) 0.5 wt.% (c) 1.5

Table 3: The variation of α(2D), α(3D), α(cr), $T^{cr\text{-}3D}$, $T^{3D\text{-}2D}$ and $T_c^{mf}$ for $(nano\text{-}Ag)_xCu_{0.5}Tl_{0.5}Ba_2Ca_2Cu_3O_{10\text{-}\delta}$, $0.0 \leq x \leq 3.0$ wt.%

| x (wt.%) | α (2D) | α (3D) | α (cr) | $T_G=T^{cr—3D}$ (K) | $T^{3D—2D}$ (K) | $T_c^{mf}$ (K) |
|---|---|---|---|---|---|---|
| **0.0** | -1.11 | -0.48 | -0.30 | 112.97 | 113.86 | 112 |
| **0.5** | -1.17 | -0.52 | -0.32 | 116.35 | 117.51 | 115.40 |
| **1.0** | -1.16 | -0.53 | -0.31 | 116.38 | 117.47 | 115.60 |
| **1.5** | -1.31 | -0.53 | -0.30 | 122.06 | 122.89 | 121.20 |
| **2.0** | -1.13 | -0.52 | -0.30 | 118.43 | 119.86 | 117.60 |
| **3.0** | -1.14 | -0.51 | -0.33 | 109.20 | 111.79 | 108.00 |

The excess conductivities Δσ was calculated as function of t in the ln-ln plot for $(nano\text{-}Ag)_xCu_{0.5}Tl_{0.5}Ba_2Ca_2Cu_3O_{10\text{-}\delta}$, for x = 0.0 for two values $T_c$ and $T_c^{mf}$ as shown in Fig. 6. This figure shows that all regions affected by the difference of these values, while Esmaeili et al. [56] found that the regions did not affect by this difference. In the rest of this paper the Δσ is calculated as function of t for $T_c^{mf}$ to avoid the arbitrary definitions of $T_c$ such as midpoint of transition curve or the temperature of the maximum of dρ(T)/dT.

Figs. 6(a), (b) and (c) show Δσ as function of t in ln-ln plot for $(nano\text{-}Ag)_xCu_{0.5}Tl_{0.5}Ba_2Ca_2Cu_3O_{10\text{-}\delta}$, for x = 0.5, 1.5 and 3.0 wt.% respectively. To compare the calculated results with the theoretical expectations, the values of α are determined from the slopes of the linearly fitting and listed in Table 3. Evidently, each plot shows three distinct regions with various values of α. Above $T_c$, the first region at greater temperature, the values of α change from -1.11 to -1.31, indicating the existence of two-dimensional fluctuations. In this region the charge carriers move in conducting $CuO_2$ planes as a result of the HTSCs layered structure. As T decreased, a crossover to second region is observed, and the α changes from −0.48 to −0.53, indicating the presence of three-dimensional fluctuations. In the 3D region the motion of the charge carriers is between the molecular planes and crossover from one plane to another. This means that the charge-carriers move with less resistivity in the whole sample before pairing (in a small range of temperature above $T_c$). The three to two dimensional crossover temperatures are computed from the intersection of the fitting lines and are recorded in Table 3. These data showed that the 3D regions shifted to higher temperatures as x increase up to 1.5 wt.% then an opposite trend was observed for higher values of x. The swing of 3D region to lower temperatures for x > 1.5 wt.% provides an evidence of the increase of addition percentage leads to a decrease in phonon population which leads to a decrease in their basic density for the electron-phonon interactions resulting to a reduction of the critical region and hence the shift in the three-dimensional region to lower temperatures. Similar result was noticed for $(Cu_{0.5}Tl_{0.5})$-1234 substituted by Cd [16]. Finally, at Ginzburg temperature ($T_G$) a crossover between 3D fluctuations and the dynamic critical fluctuations occurred. Below $T_G$, α values change from -0.30 to -0.33, which are expected from the expectation of the 3D-xyuniversality class, [57]. The E-model based on the coupling of a 2D superconducting order parameter with asymmetry-breaking field (SBF). We can see that the dimensional exponent shows a little deviation from the theoretical values given by the AL theory that could be due to the polycrystalline nature of the sample [33].

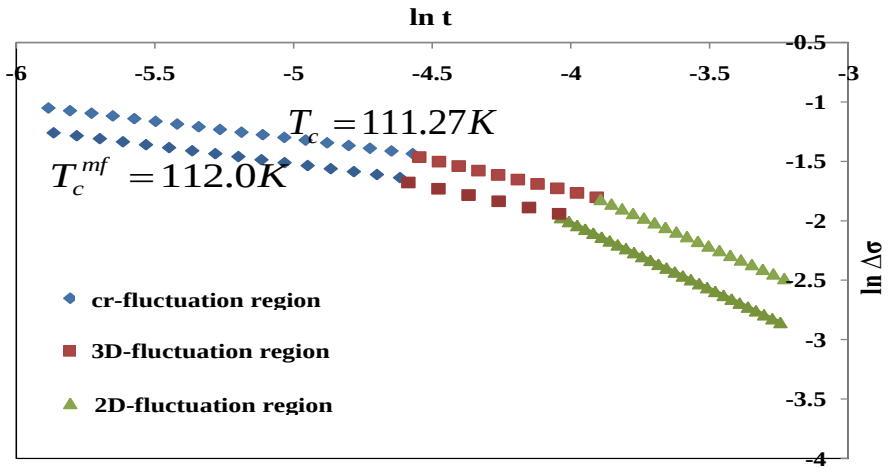


(a)

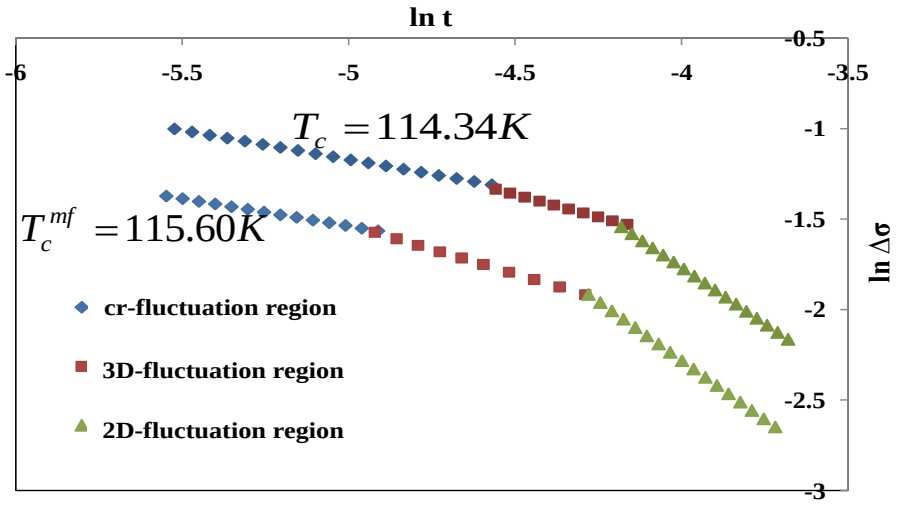


(b)

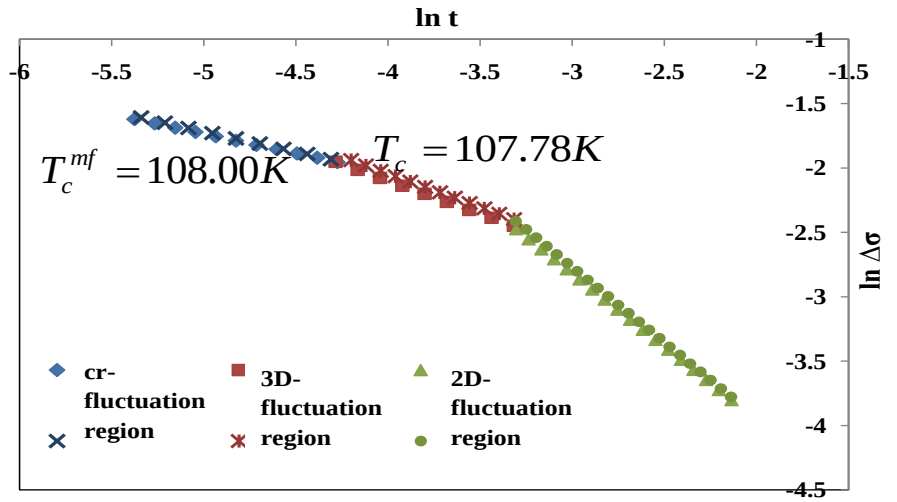


(c)

Fig. 6: The variation of Δσ with t in ln-ln plot for (nano-Ag)$_x$($Cu_{0.5}Tl_{0.5}Ba_2Ca_2Cu_3O_{10-\delta}$) for two values $T_c$ and $T_c^{mf}$: (a) 0.0 wt.%; (b) 1.0 wt.% (c) 3.0 wt.%.

$\xi_C(0)$ can be calculated from the values of $T^{3D-2D}$ for polycrystalline samples using equation (3) and their values are listed in table 4.

Table 4: Values of $\xi_C(0)$, d, $v_F$ $E_F$ and ν for (nano-Ag)$_x$$Cu_{0.5}Tl_{0.5}Ba_2Ca_2Cu_3O_{10-\delta}$, with $0.0 \leq x \leq 3.0$ wt.%

| x (wt.%) | $\xi_C(0)$ (nm) | d (nm) | $v_F \times 10^5$ (m/s) | $E_F \times 10^{-20}$ eV | $\nu \times 10^{-2}$ |
|---|---|---|---|---|---|
| **0.0** | 2.30 | 2.64 | 1.85 | 0.10 | 303.60 |
| **0.5** | 1.41 | 87.83 | 1.16 | 0.04 | 0.10 |
| **1.0** | 1.25 | 16.89 | 1.04 | 0.03 | 2.19 |
| **1.5** | 1.05 | 44.51 | 9.16 | 0.02 | 0.22 |
| **2.0** | 3.82 | 60.37 | 3.25 | 0.30 | 1.60 |
| **3.0** | 9.71 | 98.67 | 7.59 | 1.64 | 3.87 |

$\xi_C(0)$ decreases as x improves up to x = 1.5 wt.% and then reduces for further increase in x. Similar trend was noticed by Sato et al. [58] who found that the increase in Ag addition on Y-123 decreased $\xi_C(0)$. They attributed this behavior to suppression of density of the mobile carriers,

indicating that this addition changes the samples from over- to under-doped. The same behavior was observed by Mohammed [17] for $(Cu_{0.5}Tl_{0.5})$-1223 substituted by Ti and Khan et al. [15] for $(Cu_{0.5}Tl_{0.5})$-1234 substituted by Zn. The calculated values of Fermi velocity of the carriers using the equation: $v_F = \frac{5\pi k_B T_c \xi_c(0)}{2K\square}$, where $k_B$ is the Boltzmann constant and K ≈ 0.12 is coefficient of proportionality [59], are listed in table 4. The values of $v_F$ are found to be lower than that of the free electron ($v_F = 10^6$ m.s$^{-1}$). Khan et al. [60] observed similar result. The Fermi energy is determined from the relation; $E_F = \frac{1}{2} m^* v_F^2$, where $m^* \approx 10m_0$ is the effective mass of the charge carrier, $m_0$ is the carrier free mass [61] and are listed in table 4. The calculated Fermi energy are in the order of that achieved by Abou Aly et al. [62, 63] for $(Cu_{0.5}Tl_{0.5})$-1223 replaced by Presidium and Lanthanum and for (Tl,Hg)-1223 substituted by Sm and Yb. It is obvious that the Fermi energy slightly decreases by increasing nano-Ag addition till x = 1.5 wt.%. Then a reverse trend occur with x > 1.5 wt.% which could be attributed to phase change. Finally, the values of the interlayer coupling ν, which is given by $\nu = \left(\frac{2\xi_c(0)}{d}\right)^2$ [9] are listed in table 4. They are lower than 1, verifying the weak coupling between the $CuO_2$-planes and 3D-2D crossover regions [17].

## 4. CONCLUSIONS

A- In this work, the $(nano\text{-}Ag)_xCu_{0.5}Tl_{0.5}Ba_2Ca_2Cu_3O_{10-\delta}$ superconducting phase has been successfully synthesized via single step solid-state reaction technique.

B- The addition of nano-Ag to $Cu_{0.5}Tl_{0.5}Ba_2Ca_2Cu_3O_{10-\delta}$ up to x = 1.5 wt.% improved the volume fraction, grains connectivity and $T_C$. A reverse trend was observed for x > 1.5 wt.%.

C- 2D, 3D and cr fluctuations regions were clearly observed. The sample with x = 0.15 wt.% showed the lowest coherence length and Fermi velocity.

D- All the estimated values of υ are less than one confirming the weak coupling between $CuO_2$ planes and crossover between 3D and 2D regions.

## ACKNOWLEDGEMENTS

The author of the present study wish to express their thanks to the superconductivity and metallic glass lab, Physics Department, Faculty of Science, Alexandria University, Alexandria, Egypt, for aiding with the experimental procedures.

## REFERENCES

- Aslamasov, L. G., & Larkin, A. I. (1968). The Influence of Fluctuation Pairing Of Electrons on the Conductivity of Normal Metal. *Physics Letters A*, *26*(6), 238.
- Annabi, M., M'chirgui, A., Azzouz, F. B., Zouaoui, M., & Salem, M. B. (2004). Addition of nanometer Al2O3 during the final processing of (Bi, Pb)-2223 superconductors. *Physica C: Superconductivity*, *405*(1), 25.
- Abou-Aly A.I., Mohammed N.H., Awad R., Motaweh H.A., El-Said Bakeer D., (2012). Determination of Superconducting Parameters of GdBa2Cu3O7−δ Added with Nanosized Ferrite CoFe2O4 from Excess Conductivity Analysis. Journal of Superconductivity & Novel Magnetism, 25, 2281.
- Azambuja, P. D., Rodrigues Júnior, P., Jurelo, A. R., Serbena, F. C., Foerster, C. E., Costa, R. M., ... & Chinelatto, A. L. (2009). Effects of Ag Addition on Some Physical Properties of Granular YBa2Cu3O7-δ Superconductor. *Brazilian Journal of Physics*, *39*(4), 638.
- Awad, R., Abou-Aly, A. I., Gawad, M. A., & G-Eldeen, I. (2012). The Influence of Sno 2 Nano-Particles Addition on the Vickers Microhardness of (Bi, Pb)-2223 Superconducting Phase. *Journal of Superconductivity and Novel Magnetism*, *25*(4), 739.
- Awad, R., Abou-Aly, A. I., Isber, S., & Malaeb, W. (2006). Effect of the Partial Replacement of Ca by Alkaline Element Na on Tl-1223 Superconductor. In *Journal of Physics: Conference Series* (Vol. 43, No. 1, p. 474). IOP Publishing.
- Anderson, P. W., & Zou, Z. (1988). "Normal" Tunneling and" Normal" Transport: Diagnostics for the Resonating-Valence-Bond State. *Physical Review Letters*, *60*(2), 132.

- Aly, A. A., Ibrahim, I. H., Awad, R., El-Harizy, A., & Khalaf, A. (2010). Stabilization of Tl-1223 Phase by Arsenic Substitution. *Journal of Superconductivity and Novel Magnetism*, *23*(7), 1325.
- Abou-Aly, A. I., Gawad, M. A., Awad, R., & G-Eldeen, I. (2011). Improving the Physical Properties of (Bi, Pb)-2223 Phase By Sno 2 Nano-Particles Addition. *Journal of Superconductivity and Novel Magnetism*, *24*(7), 2077.
- Abou-Ali A.I., Awad R., Kamal M., Anas M., (2011). Excess Conductivity Analysis of (Cu0.5Tl0.5)-1223 Substituted by Pr and La. J. Low Temperature Physics. 163, 184
- Abou-Aly, A. I., Awad, R., Ibrahim, I. H., & Abdeen, W. (2009). Excess Conductivity Analysis for Tl0. 8Hg0. 2Ba2Ca2Cu3O9− Δ Substituted By Sm and Yb. *Solid State Communications*, *149*(7-8), 281.
- Bardeen J., Cooper L.N., Schrieffer J.R., (1957).Theory of superconductivity. Physics Review, 108, 1175
- Badica, P., Iyo, A., Crisan, A., Ishiura, Y., Sundaresan, A., & Ihara, H. (2002). (Cu, Tl) Ba2Ca3Cu4Ox compositions: I. The Influence of Synthesis Time and Temperature on the Phase Formation and Evaporation–Condensation Mechanism. *Superconductor Science and Technology*, *15*(6), 964.
- Bouchoucha, I., Azzouz, F. B., & Salem, M. B. (2011). Excess Conductivity Studies In Zn 0.95 Mn 0.05 O And Zno Added Yba 2 Cu 3 O Y Superconductors. *Journal of Superconductivity and Novel Magnetism*, *24*(1-2), 345.
- Elokr, M. M., Awad, R., El-Ghany, A. A., Shama, A. A., & El-Wanis, A. A. (2011). Effect Of Nano-Sized Zno On The Physical Properties Of (Cu 0.5 Tl 0.25 Pb 0.25) Ba 2 Ca 2 Cu 3 O 10− Δ. *Journal Of Superconductivity And Novel Magnetism*, *24*(4), 1345.
- Elsharkawy, S. G., & Awad, R. (2009). Thermal Expansion Measurements Of (Cu0. 25Tl0. 75)-1234 Added By Mgo-Nano Particles. *Journal of Alloys and Compounds*, *478*(1-2), 642.
- Esmaeili, A., Sedghi, H., Amniat-Talab, M., & Talebian, M. (2011). Fluctuation-Induced Conductivity and Dimensionality in the New Y-Based Y 3 Ba 5 Cu 8 O 18-X Superconductor. *The European Physical Journal B*, *79*(4), 443.
- Ghosh, A. K., Bandyopadhyay, S. K., Barat, P., Sen, P., & Basu, A. N. (1995). Excess-Conductivity Analysis of A Irradiated Polycrystalline Bi-2212 Superconductor. *Physica C: Superconductivity*, *255*(3-4), 319.
- Ghattas, A., Annabi, M., Zouaoui, M., Azzouz, F. B., & Salem, M. B. (2008). Flux Pinning by Al-Based Nano Particles Embedded in Polycrystalline (Bi, Pb)-2223 Superconductors. *Physica C: Superconductivity and its applications*, *468*(1), 31.
- Ganguli, A. K., Subbanna, G. N., & Rao, C. N. R. (1988). TlCaBa2Cu2O7: The 1122 (90 K) Superconductor in the New Tl (Ca, Ba) n+ 1CunO2n+ 3 series. *Physica C: Superconductivity*, *156*(1), 116.
- Gul, I. H., Amin, F., Abbasi, A. Z., Anis-ur-Rehman, M., & Maqsood, A. (2006). Effect of Ag2CO3 Addition on the Morphology and Physical Properties of Bi-Based (2223) High-Tc Superconductors. *Physica C: Superconductivity and Its Applications*, *449*(2), 139.
- Hikami S., Larkin A.I., (1988). Magnetoresistance of High Temperature Superconductors. Mod. Phys. Lett. B 2, 693.
- Han, S. H., Eltsev, Y., & Rapp, Ö. (1998). Resistive transition and fluctuation conductivity in Bi 2 Sr 2 CaCu 2 O 8+ δ single crystals. *Physical Review B*, *57*(13), 7510.
- Hohenberg, P. C., & Halperin, B. I. (1977). Theory of Dynamic Critical Phenomena. *Reviews of Modern Physics*, *49*(3), 435.
- Ihara, H., Sekita, Y., Tateai, H., Khan, N. A., Ishida, K., Harashima, E., ... & Terada, N. (1999). Superconducting properties of Cu/sub 1-x/Tl/sub x/-1223 [Cu/sub 1-x/Tl/sub x/(Ba, Sr)/sub 2/Ca/sub 2/Cu/sub 3/O/sub 10-y/] thin films. *IEEE Transactions on Applied Superconductivity*, *9*(2), 1551.
- Ihara, H., Tokiwa, K., Tanaka, K., Tsukamoto, T., Watanabe, T., Yamamoto, H., ... & Umeda, M. (1997). Cu1− xTlxBa2Ca3Cu4O12− y (Cu1− xTlx-1234) superconductor with Tc= 126 K. *Physica C: Superconductivity*, *282*, 957-958.

- Ismail, S., Yahya, A. K., & Khan, N. A. (2013). Superconducting Fluctuation and Infrared Absorption of Cd-substituted Tl0. 9Bi0. 1Sr1. 8Yb0. 2Ca1− xCdxCu1. 99Fe0. 01O7− δ Ceramics. *Ceramics International*, *39*, S257.
- Jia, Z. Y., Tang, H., Yang, Z. Q., Xing, Y. T., Wang, Y. Z., & Qiao, G. W. (2000). Effects of nano-ZrO2 particles on the superconductivity of Pb-doped BSCCO. *Physica C: Superconductivity*, *337*(1-4), 130.
- Khan, N. A., Sekita, Y., Tateai, F., Kojima, T., Ishida, K., Terada, N., & Ihara, H. (1999). Preparation of Biaxially Oriented Tlcu-1234 Thin Films. *Physica C: Superconductivity*, *320*(1-2), 39.
- Khan, N. A., Rahim, M., & Mumtaz, M. (2012). Critical regime and suppression of the pseudo-gap in Cu0. 5Tl0. 5Ba2Ca3Cu4− yZnyO12− δ superconductors via excess conductivity analyses. *Physica C: Superconductivity*, *478*, 32.
- Khan, N. A., Abbas, S., & Gardezi, S. M. H. (2013). Excess Conductivity Analysis of Tl 1− x Y x Ba 2 Ca 2 Cu 3 O 10− δ Superconductors. *Journal of Low Temperature Physics*, *172*(1-2), 70.
- Kong, W., & Abd-Shukor, R. (2010). Enhanced Electrical Transport Properties of Nano Nife 2 O 4-Added (Bi 1.6 Pb 0.4) Sr 2 Ca 2 Cu 3 O 10 Superconductor. *Journal of Superconductivity and Novel Magnetism*, *23*(2), 257.
- Khan, N. A., Saleem, A., & Hussain, S. T. (2012). Enhanced Inter-grain Connectivity in Nano-particles Doped (Cu 0.5 Tl 0.5) Ba 2 Ca 2 Cu 3 O 10− δ Superconductors. *Journal of Superconductivity and Novel Magnetism*, *25*(6), 1725.
- Khan, N. A., Khurram, A. A., Firdous, U., Ullah, S., & Khan, S. (2012). Excess Conductivity of Pb-Doped (Cu0. 5− Xpbxtl0. 5) Ba2Ca2Cu3O10− Δ Superconductors. *Physica C: Superconductivity*, *474*, 29.
- Lawrence W.E., Doniach S., (1971). Theory of Layer Structure Superconductor. *Proceedings of the 12th International Conference on Low Temperature Physics*, ed. by E. Kanda (Keigaku, Tokyo) p. 361
- Marconi, D., Pop, M., & Pop, A. V. (2012). Normal State Resistivity and Excess of Conductivity around the Optimal Doping Of Bi-2212 Thin Films. *Journal of Alloys and Compounds*, *513*, 586.
- Mohammed, N. H. (2013). The Excess Conductivity of (Cu0. 5Tl0. 5)-1223 Superconductor Substituted by Ti. *Physica C: Superconductivity*, *485*, 95.
- Mumtaz, M., Khan, N. A., Hasnain, S. M., & Ashraf, F. (2012). Superconductivity and Fluctuation-Induced Conductivity (FIC) Analysis of (Cu 0.5 Tl 0.5− x M x) Ba 2 Ca 2 Cu 3 O 10− δ. *Journal of Superconductivity and Novel Magnetism*, *25*(7), 2291-2295.
- Mohammed, N. H., Abou-Aly, A. I., Ibrahim, I. H., Awad, R., & Rekaby, M. (2011). Effect of Nano-Oxides Addition on the Mechanical Properties of (Cu 0.5 Tl 0.5)-1223 Phase. *Journal of superconductivity and novel magnetism*, *24*(5), 1463.
- Mohammed N.H., Abou-Aly A.I., Ibrahim I.H., Awad R., Roumié M., Rekaby M., (2013). Mechanical and Electrical Properties of (Cu0.5Tl0.5)-1223 Phase Added with Nano-Fe2O3. Journal of Low Temperature. Physics, 172, 234.
- Mumtaz, M., Bhatti, A. I., Nadeem, K., Khan, N. A., Saleem, A., & Hussain, S. T. (2013). Study of CuO nano-particles/CuTl-1223 superconductor composite. *Journal of Low Temperature Physics*, *170*(3-4), 185.
- Mellekh, A., Zouaoui, M., Azzouz, F. B., Annabi, M., & Salem, M. B. (2006). Nano-Al2O3 Particle Addition Effects on Y Ba2Cu3Oy Superconducting Properties. *Solid State Communications*, *140*(6), 318.
- Mohammed, N. H., Abou-Aly, A. I., Ibrahim, I. H., Awad, R., & Rekaby, M. (2009). Mechanical Properties Of (Cu0. 5Tl0. 5)-1223 Added By Nano-Sno2. *Journal of Alloys and Compounds*, *486*(1-2), 733.
- Mumtaz, M., Naeem, S., Nadeem, K., Naeem, F., Jabbar, A., Zheng, Y. R., ... & Imran, M. (2013). Study of Nano-Sized (Znfe2o4) Y Particles/Cutl-1223 Superconductor Composites. *Solid State Sciences*, *22*, 21-26.

- Martin, S., Fiory, A. T., Fleming, R. M., Schneemeyer, L. F., & Waszczak, J. V. (1990). Normal-state transport properties of Bi 2+ x Sr 2− y CuO 6+ δ crystals. *Physical Review B*, *41*(1), 846.
- Rahim, M., & Khan, N. A. (2012). Suppressed Phonon Density and Para Conductivity of Cd Doped Cu0. 5Tl0. 5Ba2Ca3Cu4− yCdyO12− δ (y= 0, 0.25, 0.5, 0.75) Superconductors. *Journal of alloys and compounds*, 513, 55.
- Saleh, S. A., Ahmed, S. A., & Elsheikh, E. M. M. (2008). A study on thermoelectric power and electrical properties of Bi-2223 superconductors sintered for different time periods. *Journal of Superconductivity and Novel Magnetism*, *21*(3), 187.

- Sedky, A. (2007). Fluctuation-Induced Excess Conductivity in R 1− x Ca x: 123 Superconductors. *Journal of Low Temperature Physics*, *148*(1-2), 53.
- Şakiroğlu, S., & Kocabaş, K. (2011). The Effect Of Silver Substitution In Bi 1.7 Pb 0.3 Sr 2 Ca 2− X Ag X Cu 3 O Y. *Journal Of Superconductivity And Novel Magnetism*, *24*(4), 1321-1325.
- Salamati, H., & Kameli, P. (2003). Effect of Deoxygenation on the Weak-Link Behavior of Yba2cu3o7− Δ Superconductors. *Solid State Communications*, *125*(7-8), 407.
- Solovjov, A. L., Habermeier, H. U., & Haage, T. (2002). Fluctuation conductivity in YBa 2 Cu 3 O 7− y films with different oxygen content. I. Optimally and lightly doped YBCO films. *Low Temperature Physics*, *28*(1), 17.
- Sato, T., Nakane, H., Yamazaki, S., & Mori, N. (2002). Analysis Of Fluctuation Conductivity In Melt-Textured Yba2cu3o7− Y Superconductors With Ag-doping. *Physica C: Superconductivity*, *372*, 1208.
- Solovjov A.L., Habermeier H.-U, Haage T., (2002). Fluctuation Conductivity In Yba2cu3ba2cu3o7−Y Films With Different Oxygen Content. II. YBCO Films With TC ≈ 80 K. Low Temperature Physics, 28, 99.
- Tokiwa, K., Tanaka, Y., Iyo, A., Tsubaki, Y., Tanaka, K., Akimoto, J., ... & Agarwal, S. K. (1998). High Pressure Synthesis and Characterization of Single Crystals of Cuba2ca3cu4oy Superconductor. *Physica C: Superconductivity*, *298*(3-4), 209.
- Takeuchi, T., Iijima, Y., Inoue, K., & Wada, H. (1997). Effect of Flat-Roll Forming On Critical Current Density Characteristics and Microstructure of Nb/Sub 3/Al Multifilamentary Conductors. *IEEE transactions on applied superconductivity*, *7*(2), 1529.
- Thompson, R. S. (1970). Microwave, Flux Flow, and Fluctuation Resistance of Dirty Type-II Superconductors. *Physical Review B*, *1*(1), 327.
- Terzioglu, C., Aydin, H., Ozturk, O., Bekiroglu, E., & Belenli, I. (2008). The Influence of Gd Addition on Microstructure and Transport Properties of Bi-2223. *Physica B: Condensed Matter*, *403*(19-20), 3354-3359.
- Varma, C. M., Littlewood, P. B., Schmitt-Rink, S., Abrahams, E., & Ruckenstein, A. E. (1989). Phenomenology of the Normal State Of Cu-O High-Temperature Superconductors. *Physical Review Letters*, *63*(18), 1996.
- Virosztek, A., & Ruvalds, J. (1990). Nested-Fermi-Liquid Theory. *Physical Review B*, *42*(7), 4064.
- Xu, Y., Hu, A., Xu, C., Sakai, N., Hirabayashi, I., & Izumi, M. (2008). Effect Of Zro2 and Zno Nanoparticles Inclusions on Superconductive Properties of the Melt-Processed Gdba2cu3o7− Δ Bulk Superconductor. *Physica C: Superconductivity*, *468*(15-20), 1363.
- Yusuf, A. A., Yahya, A. K., Khan, N. A., Salleh, F. M., Marsom, E., & Huda, N. (2011). Effect of Ge4+ and Mg2+ Doping on Superconductivity, Fluctuation Induced Conductivity and Interplanar Coupling of TlSr2CaCu2O7− δ Superconductors. *Physica C: Superconductivity*, *471*(11-12), 363.
- Zhao, B., Wan, X., Song, W., Sun, Y., & Du, J. (2000). Nano-MgO particle addition in silver-sheathed (Bi, Pb) 2Sr2Ca2Cu3Ox tapes. *Physica C: Superconductivity*, *337*(1-4), 138.